REVIEW

Fundamentals of Percolation Phenomenon with Emphasis on Its Concept in Disordered Electrochemical Systems

Kyu-Nam Jung and Su-Il Pyun[†]

Department of Materials Science and Engineering, Korea Advanced Institute of Science and Technology, 373-1 Guseong-Dong, Yuseong-Gu, Daejeon 305-701, Republic of KOREA

Abstract : This article covers the fundamentals of percolation phenomenon giving emphasis to the percolation concept involved in disordered electrochemical systems. After a brief discourse on the basic concepts of percolation theory, the geometrical properties and fractality of percolation clusters were presented. Then, anomalous behaviours of diffusion in percolation clusters were explained in terms of the fractal structures of the infinite percolation clusters. Finally, the conductivity-related properties of composite ionic materials were shortly discussed on the basis of percolation theory from practical points of view.

Key words : Percolation, Scaling law, Fractal, Anomalous diffusion, Composite ionic conductor

1. Introduction

Percolation, which is defined as the development of long-range connectivity in a random system, has been extensively studied to explain many physical phenomena in such research fields as electricity, magnetism, electrochemistry and materials science.[1-4] Since the concept of percolation was first introduced by Flory and Stockmayer[5,6] who investigated the gelation process of polymers, the knowledge of geometrical and probabilistic concepts of percolation phenomenon has been accumulated by numerous researchers.[7,8]

The basic ideas of percolation have proved to be helpful for an understanding of the principles underlying the structure and geometrical properties of colloidal particles,[9] and the diffusion/conduction process in disordered systems such as porous and amorphous materials[10-13] and composite materials.[14,15] Especially, theoretical and experimental studies on charge conduction in composite materials based upon percolation theory have recently led to considerable advance in the development of electrode and electrolyte materials for secondary rechargeable batteries and fuel cells.[16,17]

The objective of this article is to overview the fundamental aspects of percolation theory and its basic concepts in disordered electrochemical systems. Firstly, we presented the static aspects of percolation such as the geometrical properties and fractality of percolation clusters. Secondly, we discussed in detail anomalous behaviours of diffusion in the percolation clusters arising from the fractal structures of the infinite percolation clusters. Finally, we briefly described the conductivity-related properties of composite ionic materials, which are most relevant to the percolation phenomenon, from practical points of view.

[†]E-mail: sipyun@webmail.kaist.ac.kr

2. Fundamentals of Percolation Theory

2.1. Basic concepts of percolation theory

In percolation theory, a lattice is built up of sites and bonds. The simplest type of percolation system is the lattice which is purely comprised of either the site percolation or the bond percolation. Let us first consider a periodic lattice of sites in a 2-dimensional (2D) space, and assume that every site in this lattice can be in one of two states, occupied or empty. Occupied and empty sites may stand for very different intrinsic properties. Each site is randomly occupied with a probability p or is empty with a probability $(1-p)$.

Figs. 1(a) to (c) show the typical examples of the site percolation in a 2D square lattice determined at various values of p. It is seen from Fig. 1(a) that at a small value of p, e.g. $p = 0.400$, a site is either isolated or forms a small and finite cluster with nearest-neighbour sites. As the value of p increases, the average size of clusters gradually increases, and then at a certain value of p, e.g. $p = 0.593$, an infinite cluster appears which extends from one end of a lattice to the other, as demonstrated in Fig. 1(b). Such a cluster is now called the percolation cluster, and the probability at which the percolation cluster first emerges is referred to as the percolation threshold probability p_c of site occupancy. The finite and infinite clusters grow larger with further increasing p above p_c, as shown at $p = 0.700$ in Fig. 1(c).

Similarly to the case of the site percolation, one can introduce the bond percolation where a bond between two sites is randomly occupied. In the bond percolation, any of the occupied bonds belong to the same cluster, if they are connected with each other by a continuous path of the occupied bonds. At the percolation threshold probability of bond occupancy, the percolation cluster appears abruptly in a lattice. The bond
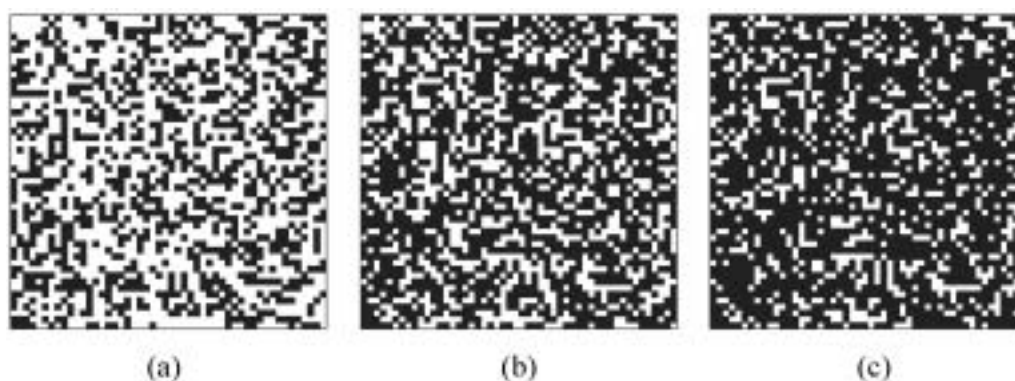
Fig. 1. Typical examples of site percolation in a 2D square lattice determined at various values of *p*: (a) *p* = 0.400, (b) *p* = 0.593, and (c) *p* = 0.700.
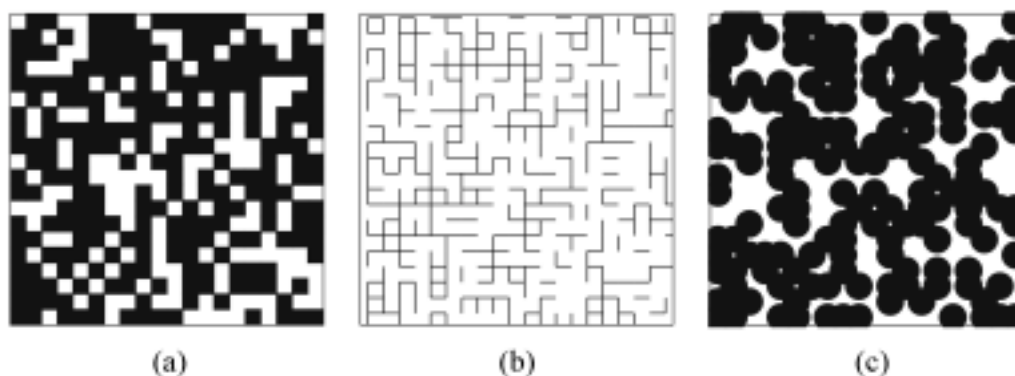

Fig. 2. Typical examples of the three kinds of percolations in a 2D lattice: (a) site percolation, (b) bond percolation, and (c) continuum percolation.

percolation concept has been mainly applied to the random resistor model for charge conduction in composite materials[1] and the gelation and polymerisation processes involved in the sol-gel synthesis.[18,19]

Considering that most of the disordered systems lack a perfect lattice structure, it seems that the position of occupied component, site or bond, may not be restricted to the discrete sites of a regular lattice. For instance, the so-called continuum percolation allows to sites or bonds overlap with one another in a uniform lattice. This percolation model has frequently been used to describe the transport phenomena in porous materials[20] and hopping conduction in doped semiconductors.[21] The three kinds of percolations described above, i.e. the site percolation, the bond percolation and the continuum percolation, are illustrated in Figs. 2(a) to (c), respectively.

It should be stressed that the infinite percolation cluster appears abruptly in a lattice at $p = p_c$. Practically, this means that the system under study has quite different intrinsic characteristics below and above p_c. As a simple example, one can consider the electrical conductivity of composite system composed of a mixture of conducting and insulating materials. In general, the transition from the insulator to the conductor occurs suddenly when the fraction of the conducting materials increases to the critical value which conceptually corresponds to p_c. In percolation phenomena, therefore, special attentions are given to the percolation threshold probability p_c.

It is well known[7,8] that the value of p_c is determined not only by the kind of occupied component, but also by the dimension and the structural details of lattice (e.g., square, triangular, etc.). The unique value of p_c can be analytically calculated for some kinds of 2D lattices in a simple manner, whereas it can be exactly evaluated for three or higher dimensional lattices, only by employing the numerical methods such as Monte Carlo simulation.[22] Table 1 summarises the typical values of p_c theoretically determined for common 2D and 3D lattices.[23]

Table 1. Typical values of the percolation threshold probabilities p_c calculated for common 2D and 3D lattices.[23]

Lattice Dimension	Lattice Type	p_c	
		Site Percolation	Bond Percolation
2	Honeycomb(Hexagonal)	0.696	0.653
	Square	0.593	0.500
	Triangular	0.500	0.347
3	Simple cubic	0.312	0.249
	Body centered cubic	0.245	0.178
	Face centered cubic	0.198	0.119

2.2. Distribution of percolation clusters and critical behaviour of percolation transition

In general, the percolation transition taking place at $p = p_c$ is closely related to the distribution and sizes of the finite clusters being present in the narrow ranges of p below and above p_c, i.e. $0 < |p - p_c| \ll 1$, which is termed the critical regime. So, it is of great importance to determine the geometrical properties of the finite and infinite clusters in the critical regime.

The most fundamental problem concerning the geometrical properties of the infinite percolation cluster is to estimate how many occupied sites belong to the infinite percolation cluster in the lattice. It is thus useful to introduce the percolation probability P_∞ which is defined as the number of occupied sites in the infinite cluster divided by the total number of occupied sites in the lattice at a given p. Since there exists no infinite percolation cluster at $p < p_c$, P_∞ should be always zero below p_c. In the critical regime, however, P_∞ increases drastically with p. Now the variation of P_∞ with p in the critical regime can approximate to the following power law:

$$P_\infty(p) \propto (p - p_c)^\beta \tag{1}$$

where β is the critical exponent for the percolation probability P_∞. The value of P_∞ approaches unity with further increasing p beyond the critical regime.

In addition to P_∞ describing the geometrical properties of the infinite cluster, now let us consider the parameters, characterising the geometrical properties of the finite clusters such as the distribution and size of the finite clusters.

The statistical distribution of the s-sized finite clusters in the lattice, where s means the number of sites in the cluster, is described in terms of the cluster density n_s. Here n_s is defined as the number of the finite clusters including s occupied sites divided by the total number of occupied and empty sites in a lattice at a given p. For a sufficiently small value of s, n_s can be calculated in a straightforward way by counting the number of permissible configurations of clusters which are called the 'lattice animals'.[7] However, for a sufficiently large value of s, the calculation of n_s becomes quite cumbersome and thus it should be helped by the computer simulation, for example, the Hoshen-Kopelman method.[24]

Remembering that the infinite percolation cluster is abruptly formed at $p = p_c$, it follows that the mean size of the finite clusters, S, diverges when p approaches p_c from below and above, and hence S may also exhibit a power law behaviour in the critical regime,

$$S(p) \propto \sum_{s=1}^{s=\infty} s n_s(p) \propto |p - p_c|^{-\gamma} \tag{2}$$

where γ is the critical exponent for the mean size of the finite clusters S. In Eq. (2), $\sum_{s=1}^{s=\infty} s n_s(p)$ simply means the fraction of occupied sites which belongs to the finite clusters in a lattice.

Practically, the size of the finite cluster is often characterised by the correlation length ξ which represents the root mean square distance between two occupied sites in the same finite cluster,

$$\xi(p)^2 = \frac{\sum_{s=1}^{s=\infty} R_s^2 s^2 n_s(p)}{\sum_{s=1}^{s=\infty} s^2 n_s(p)} \tag{3}$$

$$\text{with } R_s^2 = \frac{2 \sum_{i=1}^{i=s} \sum_{j=1}^{j=i} |r_i - r_j|^2}{s^2} \tag{4}$$

where r_i and r_j denote the positions of the ith and jth sites in the lattice, respectively. Here, it should be pointed out that ξ does not mean an average radius of the finite clusters but a maximum size of the finite clusters above which the clusters are exponentially scarce. In the same manner as does S, ξ diverges near $p = p_c$, leading to a power law behaviour in the critical regime,

$$\xi(p) \propto |p - p_c|^{-\nu} \tag{5}$$

where ν designates the critical exponent for the correlation length ξ. The typical plots of P_∞ and ξ versus p are given for a 2D square lattice at $p_c = 0.593$ in Fig. 3. The values of the critical exponents β, γ and ν are also listed for the 2D and 3D lattices in Table 2.[23] It should be noted that such critical exponents are essentially independent of the kind of occupied component and the structural details of lattice, but they depend only on the dimension of a lattice.

The physical properties associated with the percolation transition are characterised by the critical exponents β, γ and ν. A representative example of the percolation transition is the magnetic phase transition which occurs at a critical temperature T_c. In this case, the finite cluster at $p < p_c$ and the
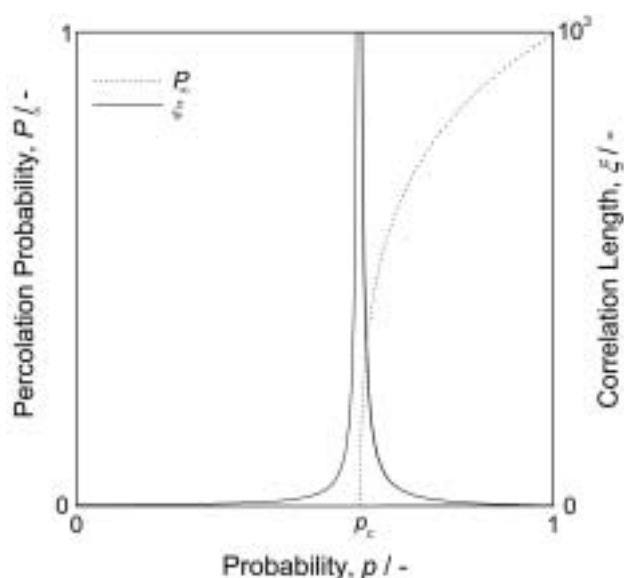

Fig. 3. Plots of correlation length $\xi(p)$ and percolation probability $P_\infty(p)$ as a function of probability p calculated for a 2D square lattice at $p_c = 0.593$.

Table 2. Typical values of the critical exponents β, γ and ν for the percolation transition calculated for 2D and 3D lattices.[23]

Critical exponent	Lattice dimension	
	2	3
β	5/36	0.4
γ	43/18	1.8
ν	4/3	0.9

infinite cluster at $p > p_c$ correspond to a disordered phase at high temperatures above T_c and an ordered phase at low temperatures below T_c, respectively. Moreover, the temperature-dependencies of Gibbs free energy, spontaneous magnetisation and susceptibility near $T = T_c$ can be satisfactorily described by the power law behaviours of n_s, P_∞ and S, respectively, in the critical regime,[8] and then such physical properties are uniquely determined by the critical exponents β, γ and ν, respectively.

3. Fractal Structure of Percolation Cluster

The structure of the infinite percolation cluster at $p \geq p_c$ can be well described by the fractal concept. Figs. 4(a) to (d) illustrate the pictures of the percolation cluster taken on different length scales.[25] From Figs. 4(a) and (b) taken on the length scales larger than ξ, it is seen that the percolation cluster has almost the compact structure, implying that the percolation cluster has just the Euclidean dimension d_E of 2. In this case, the mass M of the percolation cluster within a circle of radius R varies with R as follows:
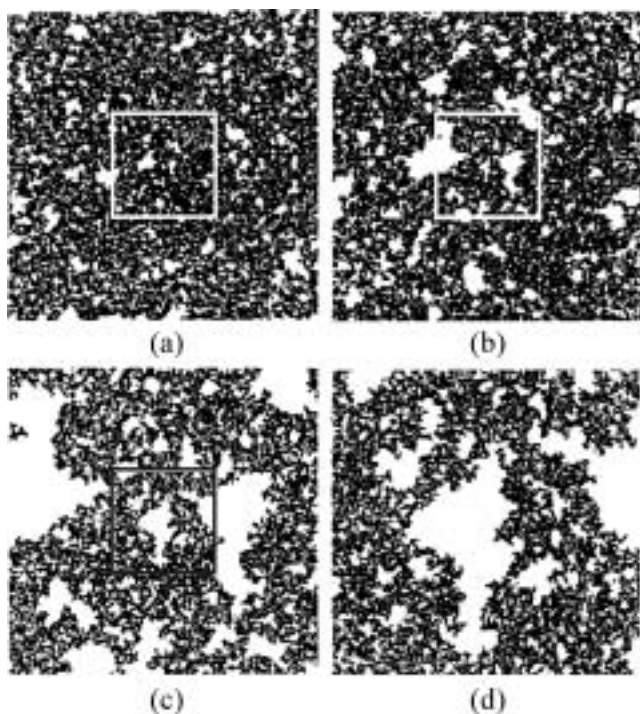

Fig. 4. The pictures of the percolation cluster taken on different length scales in a 2D square lattice; (a) and (b) : on the length scales larger than ξ, (c) and (d) : on the length scales smaller than ξ.[25]

$$M(R) \propto R^{d_E} \quad \text{for} \quad R \gg \xi \tag{6}$$

However, if one takes the pictures of the percolation cluster on the length scales smaller than ξ and then magnifies them to the original size as presented in Figs. 4(c) and (d), those pictures look almost the same: the percolation cluster is self-similar. This means that the percolation cluster itself and its surface may behave as fractals. As a result, the percolation cluster can be regarded as a mass fractal with a fractal dimension d_F on any length scale smaller than ξ. In case that the percolation cluster behaves as a mass fractal, one can then write the relationship between M and R of the cluster as

$$M(R) \propto R^{d_F} \quad \text{for} \quad R \ll \xi \tag{7}$$

The values of d_F for the percolation cluster are well known to be 1.33 for a 2D lattice and 1.9 for a 3D lattice, regardless of the structural details of the lattice.[23]

Now, one can assert that the length scale R acts as a yard-stick length for probing the mass fractal topography of the percolation cluster and at the same time the correlation length ξ corresponds just to the characteristic upper bound of R, i.e. the spatial outer cut-off of fractality, where the percolation cluster shows a fractal characteristics with self-similar scaling properties.[26-28] Here, it should be reminded that ξ diverges at $p = p_c$. This means that at $p = p_c$, the percolation cluster exhibits a fractality on all length scales.

For the case of $R \gg \xi$, M of the percolation cluster is linearly proportional to the number of the occupied sites that belong to the percolation cluster, $R^{d_E}P_\infty$, so that we obtain the following equation from Eq. (1):

$$M \propto R^{d_E}P_\infty \propto R^{d_E}(p - p_c)^\beta \tag{8}$$

In addition, M depends linearly on the number of unit cells with a size ξ, $(R/\xi)^{d_E}$, multiplied by the mass of each cell that is proportional to ξ^{d_E},

$$M \propto (R/\xi)^{d_E}\xi^{d_F} \propto R^{d_E}(p - p_c)^{\nu(d_E - d_F)} \tag{9}$$

From Eqs. (8) and (9), it follows that the mass fractal dimension d_F of the percolation cluster can be expressed in terms of the critical exponents β and ν[8]:

$$d_F = d_E - \beta/\nu \tag{10}$$

From Eq. (10), it is clear that the d_F value of the percolation cluster is always smaller than that value of d_E of the Euclidean space. This is due simply to numerous holes that exist in the percolation cluster.

The renormalisation group method, which is commonly used to determine the critical exponents, is largely based upon self-similar scaling properties of the percolation cluster at $p = p_c$. Since ξ of the percolation clusters diverges at $p = p_c$, the percolation cluster shows the self-similar properties on all length scales R, and hence one can reorganise the percolation cluster
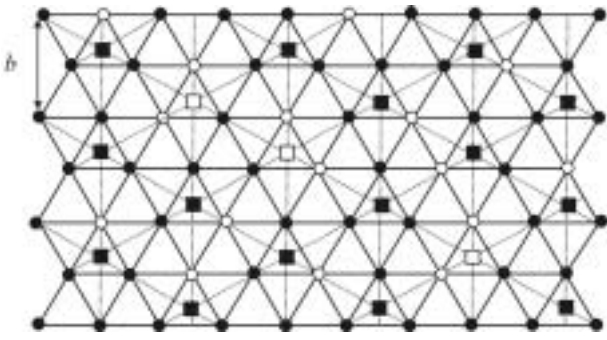
Fig. 5. Schematic diagram of the renormalization group transformation in a 2D triangular lattice. The closed and open circles represent the occupied and empty sites in an original lattice, respectively. The closed and open squares represent the occupied and empty sites in a renormalised lattice, respectively.

in a lattice by averaging over regime of size b. Such averaging procedure is called the 'renormalisation'.

Fig. 5 shows the schematic diagram of the renormalisation group transformation in a 2D triangular lattice. If one transforms a given triangular lattice by using the renormalisation group method, a site in a original lattice is replaced by a supersite in a renormalised triangular lattice, in which the lattice constant is enlarged by a factor $b = \sqrt{3}$. Here, three sites of an original lattice form the occupied supersite, when at least two sites are occupied, otherwise, the empty supersite forms. In Fig. 5, the closed and open circles denote the occupied and empty sites of an original lattice, and closed and open squares represent the occupied and empty sites of a renormlaised lattice, respectively.

In the original lattice, the correlation length ξ exhibits a power law,

$$\xi \propto \xi_{\mathrm{o}} |p - p_{\mathrm{c}}|^{-\nu} \qquad (11)$$

where ξ_{o} is the measure of the lattice constant. In the new superlattice, ξ can be also written as

$$\xi' \propto \xi'_{\mathrm{o}} |p' - p_{\mathrm{c}}|^{-\nu} \qquad (12)$$

where $b = \xi'_{\mathrm{o}} / \xi_{\mathrm{o}}$ and p' is the probability that a site in the superlattice is occupied. Since the value of the correlation length remains actually unchanged, irrespective of the renormalisation group transformation, due to the self-similar scaling property, ξ' should be equal to ξ, and hence we obtains from Eqs. (11) and (12)

$$\nu = \frac{\ln b}{\ln\left(\dfrac{p' - p_{\mathrm{c}}}{p - p_{\mathrm{c}}}\right)} \qquad (13)$$

Using the renormalization group method, the value of ν for ξ of the percolation cluster in a 2D triangular lattice is determined to be ca. 1.355, which is in good agreement with the exact value of $4/3$.[8]

4. Transport in Percolation Clusters

Keeping in mind that the percolation cluster shows a mass fractality with self-similar scaling properties, it seems evident that the physical laws of dynamics determined in the percolation cluster are quite different from those laws in a regular lattice. In particular, the diffusion and conduction processes in the percolation clusters have been extensively studied[29-31] due to a close analogy between a percolation system and a disordered system. De Gennes[32] was the first to suggest that transport in a disordered system could be successfully analysed using the random walk simulation in the percolation clusters. This random walk algorithm has been widely used to quantitatively measure the diffusivities in various disordered systems.

Now let us consider the diffusion behaviour in the finite clusters at $p < p_{\mathrm{c}}$ and the infinite percolation cluster at $p \geq p_{\mathrm{c}}$. It is generally accepted that the root mean square displacement $\sqrt{\langle r^2 \rangle}$ of a random walker acts as a yardstick length for probing the mass fractal topography of the percolation cluster during the diffusion process. For simplicity, we assume t_{ξ} as the temporal outer cut-off of fractality at which the value of $\sqrt{\langle r^2 \rangle}$ becomes comparable with the value of ξ.

At $p > p_{\mathrm{c}}$, the infinite percolation cluster has the compact and homogeneous structure for $\sqrt{\langle r^2 \rangle} \gg \xi$, and hence the value of $\langle r^2(t) \rangle$ is linearly proportional to the diffusion time t, implying the Fick's first law:

$$\langle r^2(t) \rangle \propto t \qquad \text{for } p > p_{\mathrm{c}} \text{ and } t \gg t_{\xi} \qquad (14)$$

In this case, the diffusivity D of a random walker in the percolation cluster has a constant value,

$$D(p) = \frac{\langle r^2(t) \rangle}{t} = \text{const. for } p > p_{\mathrm{c}} \text{ and } t \gg t_{\xi} \qquad (15)$$

Since the conductivity σ is characterised by a power law, $\sigma \propto (p - p_{\mathrm{c}})^{\mu}$, one gets from the Einstein relationship between σ and D and from Eq. (1) the following scaling law of D in the critical regime:

$$D(p) \propto (p - p_{\mathrm{c}})^{\mu - \beta} \qquad \text{for } p > p_{\mathrm{c}} \text{ and } t \gg t_{\xi} \qquad (16)$$

where μ is the critical exponent for the conductivity σ.

On the other hand, the infinite percolation cluster behaves as a mass fractal for $\sqrt{\langle r^2 \rangle} \ll \xi$, the diffusion law exhibits the anomalous behaviour which shows a strong deviation from the Fick's diffusion law as follows:

$$\langle r^2(t) \rangle \propto t^{2/d_{\mathrm{w}}} \qquad \text{for } p > p_{\mathrm{c}} \text{ and } t \ll t_{\xi} \qquad (17)$$

where d_{w} represents the anomalous diffusion exponent of the random walk. In general, the value of d_{w} for diffusion in the percolation cluster is theoretically determined to be larger than 2 for the ideal diffusion behaviour, which indicates that the structural disorders of the percolation cluster such as dangling ends, bottlenecks and backends slow down the movement of diffusing particles. From Eq. (16), D is given as

$$D(p) = \frac{\langle r^2(t) \rangle}{t} \propto t^{(2-d_{\mathrm{w}})/d_{\mathrm{w}}} \quad \text{for} \quad p > p_{\mathrm{c}} \text{ and } t \ll t_{\xi} \qquad (18)$$

At $p = p_{\mathrm{c}}$, the infinite percolation cluster is self-similar for all the values of $\sqrt{\langle r^2 \rangle}$ (i.e. $\xi \to \infty$ and $t_{\xi} \to \infty$), so that the anomalous diffusion described by Eqs. (17) and (18) with $d_{\mathrm{w}} > 2$ takes place over the whole range of t. Finally, at $p < p_{\mathrm{c}}$, there is no infinite percolation cluster, but all clusters in the lattice have finite sizes: the sizes of the largest finite clusters are nearly equal to ξ, and hence the value of $\sqrt{\langle r^2 \rangle}$ approaches ξ with increasing t. Therefore, from Eq. (5), one obtains the following scaling law of D in the critical regime:

$$D(p) = \frac{\langle r^2(t) \rangle}{t} \propto t^{-1} |p - p_c|^{-2\upsilon} \quad \text{for} \quad p < p_{\mathrm{c}} \text{ and } t \gg t_{\xi} \quad (19)$$

The characteristic behaviours of diffusion in the finite and infinite clusters mentioned above are clearly shown in the plots of $\log \sqrt{\langle r^2 \rangle}$ versus $\log t$ for a 2D square lattice given in Fig. 6.[7]

According to Alexander-Orbach conjecture,[33] it is assumed that the anomalous diffusion exponent d_{w} is approximately related to the mass fractal dimension d_{F} of the percolation cluster as follows:

$$d_{\mathrm{w}} \approx \frac{3}{2} d_{\mathrm{F}} \quad \text{for} \quad d_{\mathrm{E}} \geq 2 \qquad (20)$$

An interesting feature of this conjecture is that it provides a relationship between d_{w}, characterising the kinetic properties of the percolation cluster, and d_{F}, describing the static geometrical properties of the percolation cluster.

Besides the infinite percolation cluster, diffusion-limited agglomerates,[34] lattice animals,[35] and such deterministic fractal lattices as Sierpiński gasket and carpet[36] are typical examples of disordered systems for which the above-mentioned abnormalities in the diffusion behaviour have been observed.
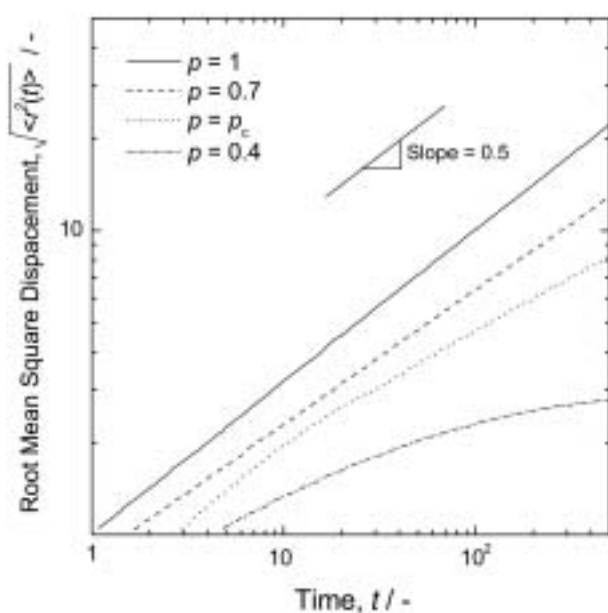

Fig. 6. Plots of log versus log t on the percolation clusters generated at various p on a 2D square lattice.[7]

5. Application of Percolation Concept to Composite Ionic Conductors

Since Liang[37] observed an enhancement of the ionic conductivity by a factor of almost 50 at a certain content of dispersed small alumina (Al_2O_3) in the matrix of lithium iodide (LiI), a substantial research has concentrated on the percolation phenomena to explain the conductor/insulator transition in dispersed ionic conductors.[37-44] Although the analytical expression for the ionic conductivity proposed by Maier[38] based upon the effective medium approximation could fit quite well to experimental results obtained from many composites of ionic conductors in a wide range of composition, it can not exactly explain the behaviour of the ionic conductivity near a critical point for the ionic conductor/insulator transition. The ionic conductor/insulator transition observed in dispersed ionic conductors was thoroughly discussed in terms of the percolation transition by Bunde et al..[39,40]

Fig. 7 shows the schematic diagrams of three-component bond percolation model for the dispersed ionic conductor proposed by Bunde et al..[41] This model is constructed by randomly selecting the occupied elementary squares with a probability p on a square lattice, which represent the insulating phase (A). The remaining empty squares correspond to the conducting phase (B). The distribution of both phases leads to a correlated bond percolation model with three types of bonds, i.e. AA-bond, BB-bond and AB-bond in the boundary between A and A, between B and B, between A and B, respectively, as illustrated in Fig. 7. Here, bond in the boundary between phases A and B represent the highly conducting component (AB-bond).
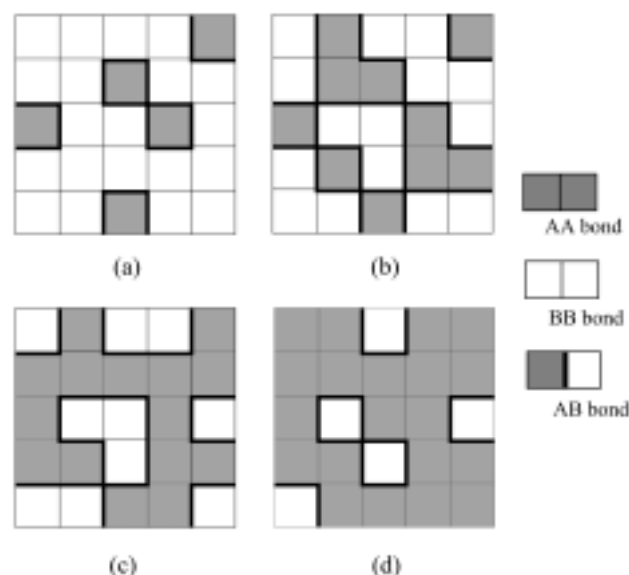

Fig. 7. Schematic diagram of a three-component percolation model for dispersed ionic conductors, for different probability p of the insulating material. The insulator phase is represented by the gray area (A), the conductor phase by the white area (B). The bonds can be highly conducting (AB-bond, bold line), normal conducting (BB-bond), or insulating (AA-bond) : (a) $p < p_{\mathrm{c}}$, (b) $p = p_{\mathrm{c}}$, (c) $p = p_{\mathrm{s}}$ and (d) $p > p_{\mathrm{s}}$.

A remarkable feature of this model is the existence of two threshold concentrations. Let us now discuss about the qualitative behaviour for the conductivity expected from Figs. 7(a) to (d). Since there are no continuous paths comprised of AB bonds from one end of lattice to the other for $p < p_c$, as shown in Fig 7(a), the current would not flow through the system. A pronounced increase of the conductivity is expected for $p = p_c$, when a macroscopic path consisting only of AB bonds is formed as shown in Fig. 7(b). However, as the value of p increases, one encounters the second critical probability $p_s = 1 - p_c$ at which the conducting bonds start forming closed loops inside the system as demonstrated in Fig. 7(c), and thus the conductivity drops drastically, leading to the conductor to insulator transition. Since there are no continuous paths comprised of AB bonds above p_s as presented in Fig 7(d), the system exhibits insulating behaviour. The values of p_c for 2D and 3D lattices were determined to be 0.41 and 0.097, respectively, by Bunde et al..[25]

However, the bond percolation model for the dispersed ionic conductor proposed by Bunde et al. is unlikely to be realistic for most systems from the following viewpoints: firstly, Bunde et al. assumed equal grain sizes of ionic conductor and insulator, although micro-sized ionic conductor particles and nano-sized insulator particles were mostly used in disordered composite materials.[42] From the numerical simulation of the conductivity behaviour in a two-dimensional system with various sizes of the insulator particles, Roman et al..[43] found that as the particle size decreases, while the thickness of the highly conducting interfacial layer is fixed, the maximum value of the conductivity appears at a smaller value of p. Next, a random distribution of ionic conductor and insulator particles was assumed in the bond percolation model by Bunde et al., but the interfacial interactions between ionic conductor and insulator particles and the smaller sizes of insulator particles lead to the formation of continuous layers of insulator around the larger conductor particles. Debierre et al.[44] reported that size of conducting component is inversely proportional to the volume fraction of insulator component by considering the interfacial interactions.

In recent times, the major interest has been manifested in commercial development of nano-sized ionic composite materials based upon the percolation model.[42,45] Indris et al.[42] have contributed substantially to the understanding of the conductivity behaviour in nano-sized ionic composite materials. They successfully described the conductivity behaviour of $Li_2O:B_2O_3$ composite material by employing the continuum percolation model.[46]

6. Concluding Remarks

The present article first explained the fundamental aspects of percolation phenomenon, including the geometrical properties and fractality of percolation clusters. Then, this article discussed in detail the abnormal diffusion behaviours of percolation clusters, which arise from the fractal structures of the infinite percolation clusters, in relation to the transport phenomenon in a disordered system. Finally, the present article briefly described the conductivity-related properties of composite ionic materials, which can be satisfactorily explained on the basis of percolation theory, from practical points of view.

Consequently, it is recognised that the percolation theory provides an effective tool to treat complex problems related to the geometrical properties and distribution of dispersed phases in disordered electrochemical systems. Especially, it is certain that the fractal characteristics of the percolation clusters and the relevant kinetic properties will be very useful for analysing atypical behaviours frequently observed in potentiostatic current transients and ac-impedance spectra from the disordered materials, e.g. porous and amorphous electrodes for secondary rechargeable batteries and fuel cells.[16,17,47,48]

References

1. S. Kirkpatrick, *Rev. Mode. Phys*, **45**, 574 (1973).
2. Y. Uemura and R. J. Birgeneau, *Phy. Rev. Lett.*, **57**, 1947 (1986).
3. C. McCall, N. Dimitrov and K. Sieradzki, *J. Electrochem. Soc.*, **148**, E290 (2001).
4. K. Malek, *Thin Solid Films*, **408**, 73 (2002).
5. P. J. Flory, *J. Am. Chem. Soc.*, **63**, 3083 (1941).
6. W. H. Stockmayer, *J. Chem. Phys.*, **11**, 45 (1943).
7. D. Stauffer and A. Aharony, "Introduction to percolation theory", Taylor & Francis, London (1992).
8. S. Havlin, A. Bunde, "Fractals and Disordered Systems", Springer Verlag, Berlin, (1996).
9. D. A. Weitz and M. Oliveria, *Phy. Rev. Lett.*, **52**, 1433 (1984).
10. D. W. Dees, T. D. Claar, T. E. Easler, D. C. Fee and F. C. Mrazek, *J. Electrochem. Soc.*, **134**, 2141 (1987).
11. G. Dumpich, St. Friedrichowski, A. Plewnia and P. Ziemann, *Phys. Rev. B*, **48**, 15332 (1993).
12. E. Bosco, *J. Electroanal. Chem.*, **366**, 43 (1994).
13. K. Aoki and Y. Teragishi, *J. Electroanal. Chem.*, **441**, 25 (1998).
14. J. Navarro-Laboulais, J. Trijueque, J.J. Garcia-Jareno, F. Vicente, *J. Electroanal. Chem.*, **399**, 115 (1995).
15. T. Kawashima and M. Hishinuma, *Mater. T. JIM*, **37**, 1397 (1996).
16. P. Costamagna, P. Costa and V. Antonucci, *Electrochim. Acta*, **43**, 375 (1998).
17. S. Mandal, J. M. Amarilla, J. Ibanez and J. M. Rojo, *J. Electrochem. Soc.*, **148**, A24 (2001).
18. H. J. Herrmann, *Phy. Rep.*, **136**, 153 (1986).
19. R. P. Pandey and Y. Liu, *J. Sol-gel Sci. Techn.*, **15**, 147 (1999).
20. Y. G. Chirkov and V. I. Rostokin, *Russ. J. Electrochem.*, **38**, 1299 (2002).
21. V. M. Aroutiounian, M. Zh. Ghoolinian and H. Tributsch, *Appl. Surf. Sci.*, **162**, 122 (2000).
22. K. Binder, *Rep., Prog. Phys.*, **60**, 487 (1997).
23. M. B. Isichenko, *Rev. Mod. Phys.*, **64**, 961 (1992).
24. J. Hoshen, R. Kopelman, *Rhy. Rev. B*, **14**, 3428 (1976).
25. A. Bunde, W. Dieterich, *J. Electroceram.*, **5**, 81 (2000).
26. H.-C. Shin, S.-I. Pyun and J.-Y. Go, *J. Electroanal. Chem.*, **531**, 101 (2002).

27. J.-Y. Go and S.-I. Pyun, *Electrochim. Acta*, **49**, 2551 (2004).

28. J.-Y. Go and S.-I. Pyun, accepted for publication in "Modern Aspects of Electrochemistry", Kluwer Academic Publishers/Plenum Publishers, New York (2005).

29. I. Webman, *Phy. Rev. Lett*., **47**, 1497, (1981).

30. S. Havlin, D. Ben-Avraham and H. Sompolinsky, *Phys. Rev. A*, **27**, 1730 (1983).

31. S. Havlin and D. Ben-Avraham, *Adv. Phys*., **51**, 187 (2002).

32. P. G. de Gennes, *La Recherche*, **7**, 919 (1976), cited in Ref. 31.

33. S. Alexander and R. Orbach, *J. Phys. (Paris)*, **43**, L625 (1982), cited in Ref. 31.

34. P. Meakin and H. E. Stanley, *Phy. Rev. Lett*., **51**, 1457 (1983).

35. S. Wilke, Y, Geffen, V. Iklovic, A. Aharony and D. Stauffer, *J. Phys. A*, **17**, 647 (1984).

36. Y. Gefen, A. Aharony and S. Alexander, *Phys. Rev. Lett*., **50**, 77 (1983).

37. C. C. Liang, *J. Electrochem. Soc*., **120**, 1289 (1973).

38. J. Maier, *J. Phys. Chem. Solids*, **46**, 309 (1985).

39. A. Bunde, W. Dieterich and H. E. Roman, *Phys. Rev. B*, **34**, 3439 (1986).

40. A. Bunde, W. Dieterich and H. E. Roman, *Solid State Ionics*, **18-19**, 147 (1986).

41. A. Bunde, W. Dieterich and H. E. Roman, *Phy. Rev. Lett.*, **55**, 5 (1985).

42. S. Indris, P. Heitjans, H. E. Roman and A. Bunde, *Phys. Rev. Lett*., **84**, 2889 (2000).

43. H. E. Roman and M. Yussouf, *Phys. Rev. B*, **36**, 7285 (1987).

44. J. M. Debierre, P. Knauth and G. Albinet, *Appl. Phys. Lett*., **71**, 1335 (1997).

45. P. Knauth, G. Albinet and J.-M. Debierre, *Solid State Ionics*, **121**, 101 (1999).

46. H. E. Roman, *J. Phys*., **2**, 3909, (1990).

47. P. Meakin and B. Sapoval, *Phys. Rev. A*, **46**, 1022 (1992).

48. D.-G. Han and G.-M. Choi, *Solid State Ionics*, **106**, 71 (1998).